A Molecular Clutch Disables Flagella in the Bacillus subtilis Biofilm

Kris M. Blair, *et al.*

Science **320**, 1636 (2008);
DOI: 10.1126/science.1157877

Science (print ISSN 0036-8075; online ISSN 1095-9203) is published weekly, except the last week in December, by the American Association for the Advancement of Science, 1200 New York Avenue NW, Washington, DC 20005.

A Molecular Clutch Disables Flagella in the *Bacillus subtilis* Biofilm

Kris M. Blair,[1] Linda Turner,[2] Jared T. Winkelman,[1] Howard C. Berg,[2,3] Daniel B. Kearns[1]*

Biofilms are multicellular aggregates of sessile bacteria encased by an extracellular matrix and are important medically as a source of drug-resistant microbes. In *Bacillus subtilis*, we found that an operon required for biofilm matrix biosynthesis also encoded an inhibitor of motility, EpsE. EpsE arrested flagellar rotation in a manner similar to that of a clutch, by disengaging motor force-generating elements in cells embedded in the biofilm matrix. The clutch is a simple, rapid, and potentially reversible form of motility control.

Many bacteria in the environment live either as motile planktonic individuals or within sessile multicellular groups called biofilms (*1*). Planktonic cells are motile owing to the presence of rotating flagella: molecular machines assembled from nearly 30 proteins (*2*). A motor, located at the base of each flagellum, uses the proton motive force to power rotation of an extracellular helical filament and propel the bacterium through the environment (*3*). In contrast, cells within a biofilm are nonmotile and aggregated by an extracellular matrix composed of secreted macromolecules (*4*). Motility and matrix synthesis are often coordinately and oppositely regulated.

In *Bacillus subtilis*, motility and biofilm formation are alternately controlled by the DNA binding transcription factor SinR (*5*). SinR represses the transcription of genes that encode the structural components of the biofilm including the *eps* operon that encodes enzymes that synthesize the matrix extracellular polysaccharide (EPS) (*6*). Cells with mutations in *sinR* constitutively derepress the *eps* genes, overproduce the matrix, and grow in sticky aggregates. We investigated why *sinR* mutants are also nonmotile (Fig. 1A).

SinR has no appreciable effect on the expression of genes required for flagellar motility (*7*). We considered the possibility that cells with mutations in *sinR* assembled flagella that were obscured by an excess of EPS and severe cell aggregation. To detect flagella within cell aggregates, we genetically altered the flagellar filament protein, Hag (*8*), such that the filament could be labeled with a fluorescent probe (Hag^{T209C}) (Fig. 1B and fig. S1). Flagella colocalized with the cell membrane in the *sinR* mutant but were unfettered when EPS biosynthesis and cell aggregation were abolished by introduction of an *epsH* mutation (Fig. 1, C and D). Nonetheless, the *sinR epsH* double mutant remained nonmotile (*sinR epsH*) (Fig. 1, A and D). Thus, the *sinR* mutant synthesized flagella that were concealed by the biofilm EPS matrix, and the flagella were also nonfunctional.

To ascertain how SinR regulates flagellar function, we genetically selected for second-site *sor* (suppressor of *sinR*) mutations that restored motility in the absence of SinR and EpsH. Eighteen spontaneous *sor* suppressor mutant strains were independently isolated, and nine of the suppressors contained mutations in the gene *epsE* (formerly *yveO*), encoding EpsE, a putative family II glycosyltransferase (*9*) (fig. S2). An artificially constructed in-frame markerless deletion of *epsE* restored motility to the *sinR epsH* mutant (*ΔepsE sinR epsH*) (Fig. 1, A and E), and motility inhibition was complemented when the *epsE* gene was cloned directly downstream of the native P_{eps} promoter and integrated at an ectopic locus [*ΔepsE* (*epsE*$^+$) *sinR epsH*] (Fig. 1A). The *epsE* gene is a member of the *eps* operon, the transcription of which is directly repressed by SinR. Thus, cells with mutations in *sinR* are nonmotile as a result of constitutive EpsE derepression.

To determine whether EpsE was sufficient to inhibit motility, we fused the *epsE* gene to an isopropyl β-D-thiogalactopyranoside (IPTG)–inducible $P_{hyspank}$ promoter and integrated the fusion at an ectopic locus (*amyE*) of an otherwise wild-type strain (*amyE::*$P_{hyspank}$*-epsE*). In the absence of induction, cells were vigorously motile (movie S1), and fluorescent staining of the Hag^{T209C}-modified filament revealed a blur of rapidly rotating flagella (movie S2). After 40 min of induction, EpsE completely inhibited cell motility (movie S3), and paralyzed flagella were clearly visible on the surface of the nonmotile cells (movie S4). Motility was similarly inhibited by an induced allele of EpsE for which a highly conserved glycosyltransferase active-site aspartate residue (*10*) was mutated to an alanine

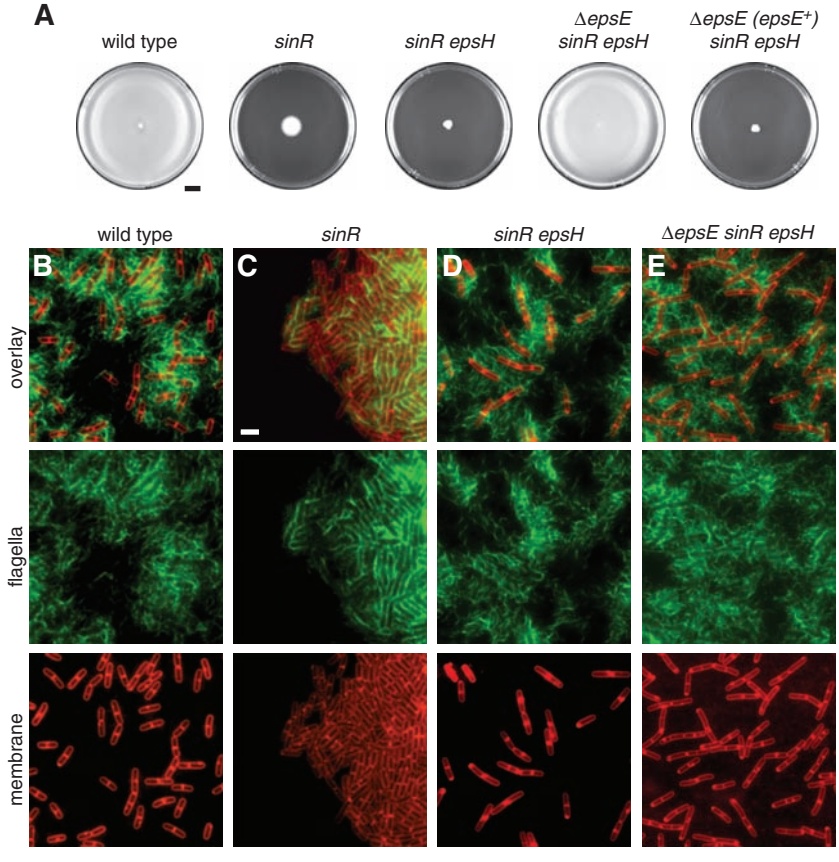

Fig. 1. EpsE is an inhibitor of motility. (**A**) Circles are top views of swarm agar Petri plates. Plates inoculated with wild-type (3610), *sinR* (DS859), *sinR epsH* (DS1674), *ΔepsE sinR epsH* (DS2946), and *ΔepsE* (*epsE*$^+$) *sinR epsH* (DS3844) were filmed against a black background such that zones of bacterial colonization appear white and uncolonized agar appears black. Motility defects are indicated as small zones of colonization. Bar, 1 cm. (**B** to **E**) Wild-type (DS1916), *sinR* (DS2198), *sinR epsH* (DS2179), and *ΔepsE sinR epsH* (DS3843) strains expressing the Hag^{T209C} construct were stained for membranes (false-colored red) and flagella (false-colored green). Bar, 2 μm.

[1]Department of Biology, Indiana University, Bloomington, IN 47405, USA. [2]Rowland Institute at Harvard, Cambridge, MA 02142, USA. [3]Department of Molecular and Cellular Biology, Harvard University, Cambridge, MA 02138, USA.

*To whom correspondence should be addressed. E-mail: dbkearns@indiana.edu

(*amyE::P*$_{hyspank}$-*epsE*^{D94A}). Thus, EpsE is sufficient to inhibit motility and does so by arresting flagellar rotation. Furthermore, the mechanism by which EpsE inhibits the flagellum is apparently unrelated to its putative enzymatic activity.

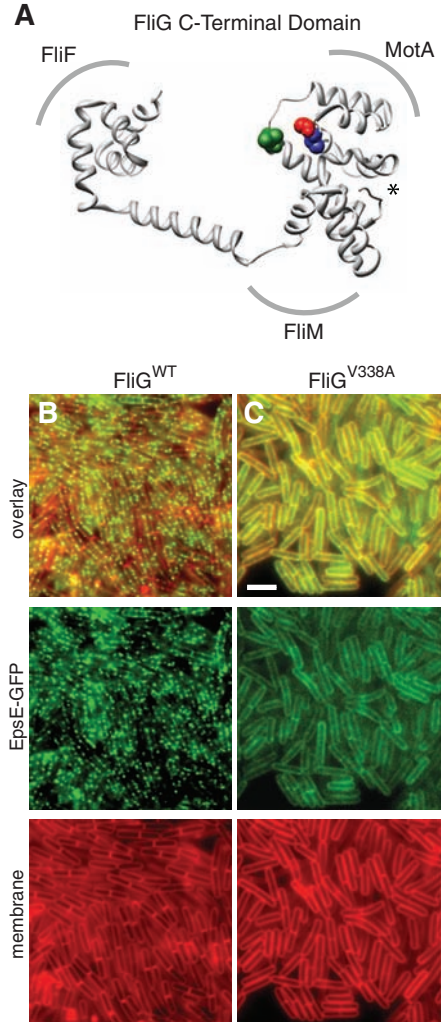

Fig. 2. EpsE interacts with the flagellar rotor. (**A**) The sites of missense mutations generated from *sorE* alleles (fig. S3) were mapped onto the published structure of FliG from *T. maritima* (*24*): Ala^{264} (blue, corresponding to *B. subtilis* FliG^{S267L}), Gly^{267} (red, corresponding to *B. subtilis* FliG^{V270G}), and Leu^{300} (green, corresponding to *B. subtilis* FliG^{L303S}). The final amino acid altered by *sorE*-class mutations FliG^{V338A} and FliG^{V338D} does not appear on the structure because the most C-terminal residue that is ordered and visible is Arg^{327} (indicated by an asterisk). The surfaces of FliG predicted to interact with FliF, MotA, and FliM are indicated by curved lines. (**B** and **C**) A strain expressing the wild-type allele of FliG (FliG^{WT}, DS2989) or *sorE10* allele of FliG (FliG^{V338A}, DS3004) was doubly mutated for *sinR* and *ΔepsE* with a complementing EpsE-GFP construct integrated at an ectopic locus. Membranes were stained with FM4-64 and false-colored in red ("Membrane"). GFP signals were false-colored in green ("EpsE-GFP"). Bar, 2 μm. Enlarged images of each panel are shown in fig. S7.

To identify the target with which EpsE interacted to inhibit flagellar rotation, we selected for spontaneous *sorE* mutations (suppressors of redundant EpsE) in the downstream cellular target that could render motility insusceptible to inhibition by EpsE. To reduce the possibility that rescue of motility mutations would disrupt the *epsE* gene itself, we expressed two copies of *epsE* on the chromosome: one at the native site by derepression due to mutation of *sinR*, and the other at the ectopic *amyE* site by induction with IPTG (*amyE*::P$_{hyspank}$-*epsE*). The *epsH* gene was mutated to eliminate EPS production that might confound mutant recovery. Twelve motile *sorE* suppressor strains were isolated from the nonmotile parent, and all 12 suppressors contained missense mutations in *fliG*.

The *fliG* gene encodes a protein that is 32% identical to the flagellar motor component FliG of *Escherichia coli*. FliG subunits polymerize into a wheel-like rotor attached to the flagellar basal body and transduce the energy of proton flux through the MotA-MotB proton channel into the rotational energy of the flagellum (*11*–*13*). The 12 different suppressors were mutated in four different residues within the C-terminal domain of FliG specifically required for torque generation (fig. S3) (*14*, *15*). Three of the four residues localized to a common surface when mapped onto the three-dimensional structure of FliG from *Thermotoga maritima* (Fig. 2A). The fourth residue, the C terminus of FliG, fell in an eight–amino acid disordered domain that might occupy a groove in the protein and potentially position the C-terminal residue near the other three suppressor sites. The surface of FliG containing the altered residues is not occluded by known interactions with the flagellum components FliF, MotA, or FliM and is a candidate site for interaction with EpsE (*16*–*18*).

To investigate whether EpsE inhibited motility through interaction with FliG, we determined the subcellular localization of EpsE translationally fused to the green fluorescent protein (GFP) and expressed under the control of the native P$_{eps}$ promoter. In cells with the *sinR* mutation, the EpsE-GFP construct was fully able to inhibit motility and when visualized by fluorescence microscopy, the EpsE-GFP fusion localized as puncta that were associated with the cell membrane, reminiscent of the sites of flagellar basal bodies (Fig. 2B). EpsE failed to localize as puncta in the presence of the FliG alleles that rendered the flagellum insusceptible to inhibition by EpsE (Fig. 2C and fig. S4). Thus, punctate localization of EpsE was required to inhibit motility, EpsE and FliG interacted in vivo, and EpsE puncta represented sites of flagellar basal bodies.

When EpsE interacts with FliG, it may cause a deflection of the FliG C-terminal domain, alter FliG interaction with MotA, and inhibit flagellar rotation in a manner similar to that of a brake or a clutch (*19*, *20*). As a brake, EpsE would jam the rotor and immobilize the flagellum. As a clutch, EpsE would disengage the rotor from the power source, but the flagellum would still be free to rotate. To distinguish these models, we tethered *B. subtilis* cells by a single flagellum and measured flagellar rotation by the counter-rotation of the cell body (*21*). Tethered motile cells rotated at a rate of about one revolution in 5 s (Fig. 3). When EpsE was induced, cell rotation was reduced but not abolished and resembled that of cells failing to express the MotA-MotB proton channel that provides the power for flagellum rotation (Fig. 3). The rotation of cells either in-

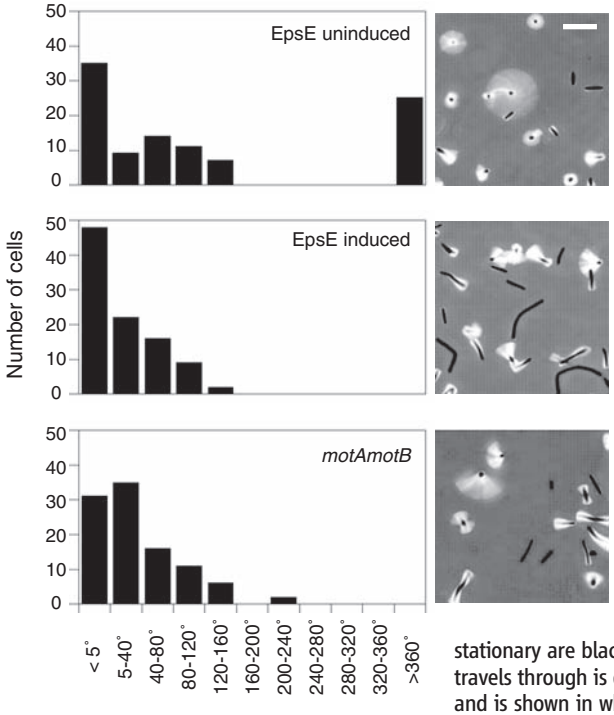

Fig. 3. When EpsE is expressed, flagella behave as though they are unpowered. Cells were tethered to microscope slides by sheared flagellar stubs, and cell rotation was monitored by video microscopy. The behavior of cells in a particular field was not uniform, and therefore 100 cells were chosen at random for motion analysis. (**Left**) The histograms indicate the number of cells that rotated through the indicated angle of rotation during a 90-s interval for "EpsE uninduced" (DS3317), "EpsE induced" (DS3317 induced with 2 mM IPTG for 2.5 hours before observation), and "*motAmotB*" (DS3318) cells. (**Right**) Each image is a time-lapse composite of a sample field corresponding to the histogram immediately to its left. Parts of the cell that are stationary are black. The range of motion that a cell travels through is depicted as a time-lapse composite and is shown in white. Bar, 10 μm.

duced for EpsE or lacking *motA* and *motB* was consistent with a calculated root mean square angular deviation of ~80° in 90 s for a *B. subtilis* cell tethered by an unpowered flagellum freely rotating by Brownian motion (supporting online material). In contrast, the angular deviation is much less, ~3°, for an *E. coli* cell tethered by an immobilized flagellum (*22*). Thus, EpsE acted as a clutch; when EpsE was induced, the flagella behaved as though they were unpowered rather than immobilized.

The biological function of the clutch appears to be related to the *B. subtilis* biofilm because *epsE* is encoded within the 15-gene *eps* operon that promotes the biosynthesis of the biofilm EPS and is repressed by SinR, the master regulator of biofilm formation. Therefore, control of a single locus ensures that cells become immobilized concomitant with biofilm formation (fig. S5A). In wild-type cells, trapped flagella and puncta of EpsE were observed within biofilm aggregates, and the cells within the aggregates were sessile (fig. S6 and movie S5). Cells expressing the $FliG^{V338A}$ clutch-insusceptible allele formed aggregates, but the cells writhed within the confines of the matrix (movie S6). We hypothesize that the clutch helps to stabilize biofilms in the environment and acts as a fail-safe mechanism to ensure that flagella do not rotate while the cells are bound by EPS.

The bacterial flagellum, powered by a motor that generates 1400 pN-nm of torque, can rotate at a frequency of greater than 100 Hz (*23*). EpsE disabled this powerful biological motor when associated with a flagellar basal body and, in a manner similar to that of a clutch, disengaged the drive train from the power source (fig. S5B). Clutch control of flagellar function has distinct advantages over transcriptional control of flagellar gene expression for regulating motility. Some bacteria, such as *E. coli* and *B. subtilis*, have many flagella per cell. The flagellum is an elaborate, durable, energetically expensive, molecular machine and simply turning off de novo flagellum synthesis does not necessarily arrest motility. Once flagellar gene expression is inactivated, multiple rounds of cell division may be required to segregate preexisting flagella to extinction in daughter cells. In contrast, the clutch requires the synthesis of only a single protein to inhibit motility. Furthermore, if biofilm formation is prematurely aborted, flagella once disabled by the clutch might be reactivated, allowing cells to bypass fresh investment in flagellar synthesis. Whereas flagellum expression and assembly are complex and slow, clutch control is simple, rapid, and potentially reversible.

References and Notes

1. R. Kolter, P. Greenberg, *Nature* **441**, 300 (2006).
2. R. M. Macnab, *Annu. Rev. Microbiol.* **57**, 77 (2003).
3. H. C. Berg, *Annu. Rev. Biochem.* **72**, 19 (2003).
4. S. S. Branda, S. Vik, L. Friedman, R. Kolter, *Trends Microbiol.* **13**, 20 (2005).
5. D. B. Kearns, F. Chu, S. S. Branda, R. Kolter, R. Losick, *Mol. Microbiol.* **55**, 739 (2005).
6. S. S. Branda, J. E. González-Pastor, S. Ben-Yehuda, R. Losick, R. Kolter, *Proc. Natl. Acad. Sci. U.S.A.* **98**, 11621 (2001).
7. F. Chu, D. B. Kearns, S. S. Branda, R. Kolter, R. Losick, *Mol. Microbiol.* **59**, 1216 (2006).
8. E. R. LaVallie, M. L. Stahl, *J. Bacteriol.* **171**, 3085 (1989).
9. P. M. Coutinho, E. Deleury, G. J. Davies, B. Henrissat, *J. Mol. Biol.* **328**, 307 (2003).
10. C. Garinot-Schneider, A. C. Lellouch, R. A. Geremia, *J. Biol. Chem.* **275**, 31407 (2000).
11. D. F. Blair, H. C. Berg, *Cell* **60**, 439 (1990).
12. S. A. Lloyd, H. Tang, X. Wang, S. Billings, D. F. Blair, *J. Bacteriol.* **178**, 223 (1996).
13. D. R. Thomas, N. R. Francis, C. Xu, D. J. DeRosier, *J. Bacteriol.* **188**, 7039 (2006).
14. V. M. Irikura, M. Kihara, S. Yamaguchi, H. Sockett, R. M. Macnab, *J. Bacteriol.* **175**, 802 (1993).
15. S. A. Lloyd, D. F. Blair, *J. Mol. Biol.* **266**, 733 (1997).
16. D. L. Marykwas, S. A. Schmidt, H. C. Berg, *J. Mol. Biol.* **256**, 564 (1996).
17. J. Zhou, S. A. Lloyd, D. F. Blair, *Proc. Natl. Acad. Sci. U.S.A.* **95**, 6436 (1998).
18. P. N. Brown, M. Terrazas, K. Paul, D. F. Blair, *J. Bacteriol.* **189**, 305 (2007).
19. S. Kojima, D. F. Blair, *Biochemistry* **40**, 13041 (2001).
20. T. Mashimo, M. Hashimoto, S. Yamaguchi, S.-I. Aizawa, *J. Bacteriol.* **189**, 5153 (2007).
21. S. M. Block, D. F. Blair, H. C. Berg, *Nature* **338**, 514 (1989).
22. S. M. Block, D. F. Blair, H. C. Berg, *Cytometry* **12**, 492 (1991).
23. N. C. Darnton, L. Turner, S. Rojevsky, H. C. Berg, *J. Bacteriol.* **189**, 1756 (2007).
24. P. N. Brown, C. P. Hill, D. F. Blair, *EMBO J.* **21**, 3225 (2002).

25. We thank N. Darnton, G. Glekas, B. Haldenwang, A. Camp, Y. Le Breton, S. Michaels, S. Mukhopadhyay, G. Ordal, and D. Rudner for reagents, constructs, and technical assistance. We thank S. Ben Yehuda, D. Blair, C. Fuqua, D. Higgins, P. Levin, R. Losick, S. Mukhopadhyay, and D. Rudner for insightful discussions and critical comments on the manuscript. This work was supported by NIH grant AI065540 (to H.C.B.) and NSF grant MCB-0721187 (to D.B.K.).

Supporting Online Material

www.sciencemag.org/cgi/content/full/320/5883/1636/DC1
Materials and Methods
SOM Text
Figs. S1 to S7
Tables S1 to S3
References
Movies S1 to S6

17 March 2008; accepted 22 April 2008
10.1126/science.1157877

Tuned Responses of Astrocytes and Their Influence on Hemodynamic Signals in the Visual Cortex

James Schummers,* Hongbo Yu,* Mriganka Sur†

Astrocytes have long been thought to act as a support network for neurons, with little role in information representation or processing. We used two-photon imaging of calcium signals in the ferret visual cortex in vivo to discover that astrocytes, like neurons, respond to visual stimuli, with distinct spatial receptive fields and sharp tuning to visual stimulus features including orientation and spatial frequency. The stimulus-feature preferences of astrocytes were exquisitely mapped across the cortical surface, in close register with neuronal maps. The spatially restricted stimulus-specific component of the intrinsic hemodynamic mapping signal was highly sensitive to astrocyte activation, indicating that astrocytes have a key role in coupling neuronal organization to mapping signals critical for noninvasive brain imaging. Furthermore, blocking astrocyte glutamate transporters influenced the magnitude and duration of adjacent visually driven neuronal responses.

Though astrocytes are the major class of nonneuronal cell in the brain (*1*), their role in brain function is unresolved. Evidence has accumulated for an active role of astrocytes in brain function (*1*–*3*). Astrocytes are closely apposed to many central synapses (*4*, *5*) and can respond to a number of neurotransmitters, including glutamate (*6*), by increases in intracellular calcium. In turn, astrocytes release glutamate and other neuroactive substances (*7*–*10*) that affect neuronal activity (*11*) and can modulate synaptic strength (*10*, *12*, *13*). Astrocytes contact vascular networks and can potentially influence the cerebral microcirculation (*14*–*16*), which has led to the proposal that astrocytes might support indirect, hemodynamic imaging of neuronal activity (*17*, *18*). Despite these in vitro studies, however, little is known about the behavior of astrocytes in vivo. Pioneering studies have demonstrated that astrocytes do respond to neural activity in vivo (*19*–*21*), but fundamental questions about the relationship between neuronal networks, astrocytes, and hemodynamic responses remain unsolved.

The precise orderly mapping of orientation preference in the visual cortex of higher mammals provides a model system with which to study these interactions. The synaptic input near pinwheel centers is nearly untuned (*22*), yet individual neurons are sharply tuned because of nonlinear filtering of inputs (*23*) and are organized on a scale of less than 50 μm (*24*). Do astrocyte responses passively follow the untuned

Picower Institute for Learning and Memory, Department of Brain and Cognitive Sciences, Massachusetts Institute of Technology, Cambridge, MA 02139, USA.

*These authors contributed equally to this work.
†To whom correspondence should be addressed. E-mail: msur@mit.edu